NASA TECHNICAL NOTE

NASA TN D-7926 C.1

NASA TN D-7926

ANALYTICAL AND EXPERIMENTAL INVESTIGATION
OF FATIGUE IN A SHEET SPECIMEN WITH
AN INTERFERENCE-FIT BOLT

John H. Crews, Jr.

Langley Research Center
Hampton, Va. 23665

NATIONAL AERONAUTICS AND SPACE ADMINISTRATION • WASHINGTON, D. C. • JULY 1975

1. Report No. NASA TN D-7926	2. Government Accession No.	3. Recipient's Catalog No.	
4. Title and Subtitle ANALYTICAL AND EXPERIMENTAL INVESTIGATION OF FATIGUE IN A SHEET SPECIMEN WITH AN INTERFERENCE-FIT BOLT		5. Report Date July 1975	
		6. Performing Organization Code	
7. Author(s) John H. Crews, Jr.		8. Performing Organization Report No. L-10067	
9. Performing Organization Name and Address NASA Langley Research Center Hampton, Va. 23665		10. Work Unit No. 505-02-31-01	
		11. Contract or Grant No.	
12. Sponsoring Agency Name and Address National Aeronautics and Space Administration Washington, D.C. 20546		13. Type of Report and Period Covered Technical Note	
		14. Sponsoring Agency Code	

15. Supplementary Notes

16. Abstract

A fatigue analysis, based on finite-element calculations and fatigue tests, was conducted for a 7075-T6 aluminum-alloy sheet specimen with a steel interference-fit bolt. The stress analysis of the region near the bolt hole showed that the beneficial effect of an interference-fit bolt can be interpreted as the combined result of two effects — the first caused by load transfer through the bolt and the second caused by the compressive interference stresses in the sheet.

As expected, the fatigue tests showed that progressively higher interference levels produced longer fatigue lives. But, these tests also showed that a high level of interference prevented fretting at the bolt-sheet interface and that interferences larger than this level produced little additional improvement in fatigue life.

When stress-life (SN) curves were plotted on the conventional basis of net-section nominal stress, portions of the curves for interference-fit specimens were found to lie above the unnotched specimen curve that is the logical upper limit for fatigue improvement. This behavior was explained in terms of the load transferred through the bolts by the loaded specimen. Comparisons based on nominal net-section stress do not account for this load transfer and therefore exaggerate the beneficial effects of interference-fit bolts.

17. Key Words (Suggested by Author(s)) 7075-T6 aluminum-alloy sheet Elastoplastic finite-element analysis Fatigue lives Fretting Interference-fit bolt	18. Distribution Statement Unclassified — Unlimited New Subject Category 39		
19. Security Classif. (of this report) Unclassified	20. Security Classif. (of this page) Unclassified	21. No. of Pages 29	22. Price* $3.75

ANALYTICAL AND EXPERIMENTAL INVESTIGATION OF FATIGUE IN A
SHEET SPECIMEN WITH AN INTERFERENCE-FIT BOLT

John H. Crews, Jr.
Langley Research Center

SUMMARY

A fatigue analysis, based on finite-element calculations and fatigue tests, was conducted for a 7075-T6 aluminum-alloy sheet specimen with a steel interference-fit bolt. The stress analysis of the region near the bolt hole showed that the beneficial effect of an interference-fit bolt can be interpreted as the combined result of two effects — the first caused by load transfer through the bolt and the second caused by the compressive interference stresses in the sheet.

As expected, the fatigue tests showed that progressively higher interference levels produced longer fatigue lives. But, these tests also showed that a high level of interference prevented fretting at the bolt-sheet interface and that interferences larger than this level produced little additional improvement in fatigue life.

When stress-life (SN) curves were plotted on the conventional basis of net-section nominal stress, portions of the curves for interference-fit specimens were found to lie above the unnotched specimen curve that is the logical upper limit for fatigue improvement. This behavior was explained in terms of the load transferred through the bolts by the loaded specimen. Comparisons based on nominal net-section stress do not account for this load transfer and therefore exaggerate the beneficial effects of interference-fit bolts.

INTRODUCTION

Numerous studies have demonstrated that longer fatigue lives are obtained by using interference-fit bolts rather than clearance-fit bolts. Most of these studies, however, have included factors that either influence the fatigue results or complicate the analysis of the results. Such factors are countersunk bolt holes, complex joint configurations, bolt clamp-up, fretting between faying surfaces, or variable-amplitude loading. These complications were purposely avoided in the present study, because its purpose was to analyze the basic influence of interference bolts on fatigue life.

The case analyzed in the present study consisted of a steel interference-fit bolt in an aluminum-alloy sheet specimen (7075-T6) under constant-amplitude uniaxial loading.

Fatigue tests were conducted to determine lives for ranges of interference and load levels typical of those in aircraft structures. The test specimen was analyzed by a finite-element procedure which was developed in reference 1 but was modified in the present study to account for the finite width of the specimen.

The fatigue critical stresses near an interference-fit bolt were compared with the corresponding stresses for a clearance-fit bolt. The comparison revealed how the stress fields associated with interference-fit bolts helped prolong fatigue life. The test results, presented as fatigue lives and as locations for crack initiation and fretting at the bolt holes, were analyzed using the finite-element results.

SYMBOLS

D	diameter of bolt hole, m
E	Young's modulus, Pa
I	interference, difference between bolt and hole diameters, m
N	fatigue life, cycles
r, θ	polar coordinates, m and deg
R	ratio of minimum to maximum stress
S	nominal net-section stress, Pa
x, y	Cartesian coordinates, m
ΔP	change in interference bolt head protrusion, m
ϵ	uniaxial strain
μ	coefficient of friction
σ	uniaxial stress, Pa
σ_n	normal stress on plane of largest alternating shear stress, Pa
$\sigma_{rr}, \sigma_{\theta\theta}$	normal stress components in polar coordinates, Pa

σ_{xx}, σ_{yy} normal stress components in Cartesian coordinates, Pa

τ shear stress on plane of largest alternating shear stress, Pa

τ_a alternating shear stress on plane of largest alternating shear stress, Pa

$\tau_{r\theta}$ shear stress component in polar coordinates, Pa

Subscripts:

int   interference

min   minimum

max   maximum

ANALYTICAL INVESTIGATION

The specimen configuration shown in figure 1 was analyzed. Results are presented as stress distributions near the bolt hole and as interference-loading combinations which correspond to the onset of slip and separation. The stress distributions were calculated for one combination of interference and loading: $I = 0.10$ mm, $S_{max} = 275$ MPa, and $S_{min} = 14$ MPa $(R = 0.05)$. As is shown later, this combination produced neither slip nor separation. The severity of the cyclic biaxial stresses near the bolt hole was evaluated by a fatigue analysis. The results from these calculations are used to interpret the fatigue test results.

Stress Analysis

Finite-element procedure.- The finite-element procedure was like that used in reference 1 to analyze a wide sheet with an interference-fit bolt. The procedure was based on a finite-element computer program formulated for elastoplastic plane-stress elements that had either uniform strains or linearly varying strains. This program, described in references 2 and 3, calculated the onset of plasticity by the von Mises yield criterion and then calculated subsequent plastic response by an incremental loading approach. The program was modified so that the specimen could be analyzed for sequential bolt insertion and specimen loading. Because plasticity is involved, the stress distributions depend on which operation occurs first.

The finite-element model of the specimen is shown in figure 2(a). Because of symmetry, a one-quadrant model is adequate. It has small linearly varying strain elements

near the bolt hole and uniform strain elements elsewhere. The finite-element model in figure 2(b) represented the bolt. The bolt model, equal in thickness to that of the sheet, was connected to the sheet model at all nodes along their interface. Interference between the bolt and sheet was simulated by expanding the small hole at the bolt center; the bolt stiffness was assumed to be unaffected by this hole.

The stress-strain curve for the 7075-T6 sheet specimen was approximated by the Ramberg-Osgood equation (ref. 4) in figure 3. The steel bolt was assumed to have an elastic modulus of 207,000 MPa and a yield strength high enough to preclude yielding. Poisson's ratio was taken as 0.3 for both the sheet and the bolt.

Stress distributions.- The stress distributions along the X-axis are presented in figure 4(a). They are shown as dashed curves for bolt insertion, as solid curves for maximum load, and as dash-dot curves for minimum load. These three conditions are also indicated by the subscripts int, max, and min, respectively.

The vertical lines in figure 4(a) show the extent of the yield zone at the X-axis. Bolt insertion yielded the sheet to $x/D = 0.8$; then the loading to S_{max} extended this zone to $x/D = 1.2$. Although not obvious from this figure, unloading from S_{max} to S_{min} produced only elastic changes in the local stresses. Consequently, the subsequent cyclic loading between S_{min} and S_{max} also produced only elastic stress excursions. The σ_{yy} at the hole boundary alternated between 50 and 150 MPa; this local stress range corresponds to a stress concentration factor of 0.40, based on net-section nominal stress range. Because a finite-width sheet was used in the present analysis, this value is slightly smaller than the theoretical elastic value of 0.45 for an infinite sheet (ref. 5). The 0.40 value is much smaller than the 2.48 stress concentration factor for a sheet with a clearance-fit bolt (open hole) and the same finite width (ref. 6). This comparison shows the extent by which an interference-fit bolt can reduce the stress concentration at a bolt hole.

The influence that an interference-fit bolt has on the stress concentration at a bolt hole can be explained in terms of the load transfer near the bolt hole when the sheet is loaded. If the hole is open or contains a clearance-fit bolt, load in the sheet cannot transfer across the bolt hole but must "deflect" around the hole. This deflected portion of the load causes the stress concentration. In contrast, if the hole contains an interference-fit bolt, load passes through the bolt. Therefore, the hole deflects less load and consequently causes a smaller stress concentration.

Evidence of load transfer through the bolt is shown in figure 4(b) which presents the stress distributions along the hole boundary. The σ_{rr} and $\tau_{r\theta}$ stresses in this figure act on the bolt-sheet interface; thus changes in their values for the S_{min} to S_{max} loading would indicate that some load transferred through the bolt. The differences between $(\sigma_{rr})_{max}$ and $(\sigma_{rr})_{min}$, largest near $\theta = 90^\circ$, indicate that a portion of the

4

applied cyclic load transferred through the bolt by decreasing the compressive loading on the bolt. The differences between $(\tau_{r\theta})_{max}$ and $(\tau_{r\theta})_{min}$, largest near $\theta = 45^\circ$, indicate that an additional portion of the applied load transferred through the bolt by increasing the shear loading on the bolt. The total load transferred through the bolt was calculated to be approximately 20 percent of the applied load on the specimen for the case considered in figure 4(b).

The load transfer through the bolt had an additional effect which should be mentioned. Because about 20 percent of the applied load passed through the bolt, only the remaining 80 percent of the applied load acted on the net section of the specimen. Consequently, the nominal net-section stress, calculated as the applied load divided by net-section area, was larger than the average net-section stress. For the case analyzed the nominal net-section stress was 275 MPa, but the actual average net-section stress was only 220 MPa. Later discussions will show that comparisons of fatigue results from different specimen configurations can be misleading if results are compared on the basis of nominal net-section stress.

Although not evident in figure 4(b), during the remote loading the principal stress directions rotated (except for $\theta = 0^\circ$ and 90°). Bolt insertion produced symmetric stresses around the hole and therefore radial and tangential principal stress directions; but, when the remote stress S_{max} was applied (in the Y-direction), the principal stress directions rotated toward the X- and Y-directions. For subsequent loading between S_{min} and S_{max}, the principal stress directions rotated cyclically. This cyclic rotation, largest on the hole boundary near $\theta = 45^\circ$, is discussed further in the fatigue-analysis section.

Slip and separation.- Slip and separation were analyzed because each was expected to be detrimental to fatigue life. Both slip and separation reduce the bolt's effectiveness because they reduce the load transferred through the bolt. Cyclic slip can also cause fretting damage at the interface.

The onset of slip was established by the following procedure. As the applied load was increased incrementally in the finite-element program, the interface shear stress $\tau_{r\theta}$ was compared with the friction stress $\mu\sigma_{rr}$, where μ is the coefficient of friction and σ_{rr} is the normal stress on the interface. Slip was assumed to occur when $\tau_{r\theta} = \mu\sigma_{rr}$ ($\mu = 0.4$ on p. 366 in ref. 7).

The applied stresses necessary for separation were calculated by increasing the load in the finite-element analysis until the contact stress equaled zero at $\theta = 90^\circ$, the point of initial separation. Although slip would occur before separation, a no-slip interface was assumed because this analysis could not account for postslip behavior. Consequently, the calculated separation levels represent an upper bound; slip would allow separation at lower stress levels.

Figure 5 presents the slip and separation curves for a range of interference values. This figure indicates that neither slip nor separation occurred for the case analyzed in figure 4. Figure 5 shows that the fatigue-test combinations of applied stress and interference span the full range of behavior — no slip, slip, and separation.

Fatigue Analysis

The purpose of this section is to analyze the mechanism responsible for the longer fatigue lives attained when interference-fit bolts are used rather than clearance-fit bolts. The approach used is based on a comparison of the severity of stresses near holes with interference-fit and clearance-fit bolts.

The biaxial fatigue analysis used here was based on the hypothesis that fatigue is governed by alternating shear stress and the maximum normal stress acting on the shear stress plane (refs. 8 and 9). As mentioned previously, the principal-stress planes rotated during cyclic loading. To account for this rotation the procedure in reference 10 was used. First, for each local stress state, the plane was determined for which the alternating shear stress was largest. Then, the shear and normal stresses on this plane were calculated for the S_{max} and S_{min} loadings.

The calculated shear stress τ and normal stresses σ_n for the planes of largest alternating shear stress are presented in figure 6. These stresses are presented for both the X-axis (fig. 6(a)) and the hole boundary (fig. 6(b)) because test results from reference 11 and the present study indicate that fatigue cracks may initiate in either of these regions. As mentioned previously, the alternating shear stress τ_a, where $\tau_a = (\tau_{max} - \tau_{min})/2$, and the maximum normal stress $(\sigma_n)_{max}$ were assumed to govern fatigue. Accordingly, crack initiation was assumed to occur where the combination of τ_a and $(\sigma_n)_{max}$ was most severe.

Because the most severe combination of τ_a and $(\sigma_n)_{max}$ in figure 6 is not obvious, the severity of these stresses was established by comparing them with fatigue data (ref. 11), as shown in figure 7. The solid curve represents the calculated combinations of τ_a and $(\sigma_n)_{max}$ for points along the X-axis. The dashed curves represent constant-life data for the stresses on the $\pm 45^\circ$ shear planes in unnotched specimens (ref. 11). These constant-life curves were interpreted as "constant-fatigue-severity" curves and were used to evaluate the severity of the calculated stresses. Figure 7 shows that the cyclic stresses on the X-axis are most severe in the region $1.10 \leq x/D \leq 4.46$ (specimen edge). Figure 8 compares the stresses on the hole boundary with the constant-life curves and shows that the most severe stress state occurs at $\theta = 50^\circ$.

A comparison of figures 7 and 8 indicates that the stresses are more severe on the X-axis than along the hole boundary; however, the difference between the stress severities for the X-axis and the hole boundary is small. And, as previously mentioned, for the present study the fatigue cracks often initiated at the hole boundary. For these reasons, the fatigue critical locations on both the hole boundary and the X-axis were considered in subsequent analyses.

The mechanism responsible for the longer fatigue lives obtained with interference-fit bolts than with clearance-fit bolts was analyzed by comparing the fatigue critical stresses in sheets with these two types of bolts. The critical stresses for the interference-fit case were taken from figures 7 and 8 for $x/D \geqq 1.10$ and $\theta = 50^{\circ}$, respectively. The corresponding critical stresses for the clearance-fit case were calculated for the boundary of an open hole at $\theta = 0^{\circ}$. The stresses are compared in the following table:

	Interference fit		Clearance fit
	X-axis at $x/D \geqq 1.10$	Hole boundary at $\theta = 50^{\circ}$	Hole boundary at $\theta = 0^{\circ}$
τ_a, MPa	50	70	160
$(\sigma_n)_{max}$, MPa	170	80	270

This comparison shows that the τ_a and $(\sigma_n)_{max}$ values for both critical locations in the interference-fit case are smaller than the corresponding stresses for the clearance-fit case.

The differences between the critical τ_a and $(\sigma_n)_{max}$ values for the interference-fit and clearance-fit cases were caused by a combination of two effects. First, as previously discussed, load transfer through an interference-fit bolt causes the local stress ranges to be smaller than for the clearance-fit case. This load-transfer effect causes smaller τ_a values and also lowers the $(\sigma_n)_{max}$ values. Second, the interference-fit bolt induces larger compressive interference stresses near the bolt hole, and these stresses lower the $(\sigma_n)_{max}$ values. Although these two effects were not analyzed quantitatively, both are believed to prolong fatigue life. This belief is in contrast to the general opinion that the load-transfer effect is the sole cause for the longer lives associated with interference-fit bolts. It should be noted that these two effects are governed by different interference-fit parameters. The load-transfer effect depends primarily on the bolt-to-sheet stiffness ratio, whereas the intereference-stress effect depends on the level of interference.

FATIGUE TESTS

Test Procedure

Figure 1 shows the fatigue specimen with an installed bolt — a tapered bolt pulled into a tapered hole, producing an interference fit. The interference level was controlled by measuring the bolt-head protrusion — first with the bolt inserted under a light load (about 20N) and again after the bolt was pulled into the hole. Interference and change in protrusion ΔP were related by $I = \Delta P/48$ (ref. 12).

Because the purpose of the fatigue tests was to demonstrate the basic effect of an interference fit, precautions were taken to eliminate other effects that could alter the fatigue results or could complicate the analysis of results. For this reason, the tests were conducted with a simple specimen configuration and constant-amplitude uniaxial loading. Fretting under the bolt head and bolt clamp-up effects were avoided by not pulling the bolt head into contact with the specimen. A thin Teflon washer prevented fretting under the nut. No special attempt was made, however, to prevent fretting in the bolt hole. The bolts were used in their "as-received" condition, that is, with cadmium plating and cetyl alcohol lubricant (ref. 12).

Fatigue tests were conducted for ranges of both interference and cyclic load. Fatigue lives, crack-initiation sites, and fretting marks in the bolt holes are discussed from the viewpoint of analyses in the previous section.

Test Results

Fatigue lives.- Figure 9 presents fatigue lives for $S_{max} = 275$ MPa and a range of interference levels. Each symbol represents the median of four test lives (table 1). As expected, larger interference levels produced larger fatigue lives. The life for $I = 0.10$ mm is about 100 times that for the clearance-fit (open-hole) case, but for $I > 0.10$ mm little additional improvement is shown. This trend correlates with the absence of slip for $I > 0.10$ mm.

Figure 10 shows a comparison of fatigue lives for $I = 0.05$ mm and $I = 0.10$ mm with lives for open-hole and unnotched specimens. Again the symbols represent median lives (see tables 2, 3, and 4). The unnotched specimen curve in this figure is the logical upper limit for the fatigue lives of specimens with interference-fit bolts, but portions of the $I = 0.05$-mm and $I = 0.10$-mm curves are seen to lie above this limit. This paradox developed because these curves were compared on the conventional basis of nominal net-section stress. As previously mentioned, nominal stresses do not account for the load transfer through interference-fit bolts. Although a portion of the applied load transfers through the bolt and therefore only the remaining portion of the load acts on the net section of the specimen, the nominal stresses in this figure were calculated on the usual assump-

8

tion that all of the applied load acted on the net section. As a result, the interference-fit curves in figure 10 are plotted at nominal stress levels that are larger than the average net-section stresses actually present during the fatigue tests. If the interference-fit curves were plotted for average net-section stresses, these curves would probably lie below the unnotched curve, as expected. Unfortunately, these average net-section stresses could not be calculated because the effects of slip and separation on load transfer through the bolt were not accounted for by the present finite-element analysis.

To compare the curves in figure 10 on an equal-stress basis, they were replotted in figure 11 in terms of gross-section nominal stress. On the basis of gross-section nominal stress, the interference-fit curves lie below the curve for unnotched specimens, as expected. Comparison of the $I = 0.05$-mm and $I = 0.10$-mm curves with that for open-hole specimens shows that the interference-fit bolts improved fatigue lives by a factor of about 10 and raised the fatigue limit by approximately 70 MPa.

Crack initiation and fretting.- The fracture surface of each fatigue specimen was examined to locate the crack-initiation site, and the bolt hole was examined for evidence of fretting. Figure 12(a) shows typical locations for cracks and fretting marks. These marks were symmetrically located and were usually well-defined regions about 20° to 40° wide. Figure 12(b) shows a sketch of a typical fracture surface.

Figure 12(c) presents results for a range of interference levels with $S_{max} = 275$ MPa (table 1). For $I = 0$ the cracks started near $\theta = 0^O$, as in specimens with open holes. But for $I = 0.025$ mm, they initiated near $\theta = 50^O$, and for $I = 0.10$ mm (the case analyzed) cracks initiated between $\theta = 25^O$ and 45°, compared to the most critical hole boundary location of $\theta = 50^O$ from the analysis in figure 8. For interference levels larger than $I = 0.10$ mm the cracks usually started near $\theta = 30^O$, but in several cases they started on the outer edge of the specimen.

Figure 12(c) also shows the locations for the midpoints of the fretted regions. For the low interference levels the cracks initiated in the fretted regions; this observation indicates that fretting probably shortened fatigue lives for these interference levels. However, fretting marks were not found for $I \geqq 0.10$ mm; this result corroborates the prediction that slip would not occur for $I \geqq 0.10$ mm.

The influence of applied stress level on crack initiation and fretting locations is shown in figures 12(d) and 12(e). For $I = 0.05$ mm (fig. 12(d)) fretting marks were observed over the entire range of applied stress. In most cases the cracks initiated within the fretted regions, indicating that fretting probably influenced the fatigue lives for this interference level. In contrast, for $I = 0.10$ mm figure 12(e) indicates that fretting occurred only for $S_{max} \geqq 350$ MPa and also shows that the fretting and crack initiation locations were widely separated. Thus, fretting probably did not shorten the fatigue lives for $I = 0.10$ mm.

CONCLUDING REMARKS

A fatigue analysis, based on finite-element calculations and fatigue tests, has been conducted for a 7075-T6 aluminum-alloy sheet specimen with a steel interference-fit bolt. The fatigue-test results were analyzed in terms of stresses near the bolt hole and in terms of slip at the bolt-sheet interface.

The stress analysis of the region near the bolt hole showed that the principal shear-stress planes rotated during cyclic loading of the specimen. As a result, the biaxial fatigue analysis was based on stresses calculated for the planes of largest alternating shear stress. This analysis indicated that the two most fatigue-critical areas were on the transverse axis at a distance of about one radius from the hole and on the hole boundary at about 50° from the transverse axis. A comparison of the stresses at these two points with the corresponding critical stresses for the open-hole case indicated that the beneficial effect an interference bolt has on fatigue life can be interpreted as the combined result of two separate effects. First, the load transfer through an interference-fit bolt causes the alternating stresses near the bolt hole to be smaller than for the open-hole case. Second, the compressive stresses induced by the interference fit reduce the normal stresses on the critical shear planes.

As expected, the tests with a single level of maximum applied stress (275 MPa) showed that higher interference levels produced longer fatigue lives. These tests also showed that a high interference level prevented fretting at the bolt-sheet interface and that interferences above this level produced little additional improvement in fatigue life. The interference level found necessary to prevent fretting in the tests correlated closely with the calculated interference level necessary to prevent slip at the bolt-sheet interface.

Portions of the stress-life (SN) curves for specimens with interference-fit bolts were found to lie above the unnotched specimen curve that is the logical upper limit for fatigue improvement. The explanation for this behavior is that the curves were compared on the conventional basis of net-section nominal stress, which does not account for the load that passes through the bolts when the specimens are loaded. When compared on the basis of gross-section nominal stress, the SN curves for the specimens with interference-fit bolts were shown to lie below the curve for unnotched specimens, as expected.

Langley Research Center,
    National Aeronautics and Space Administration,
        Hampton, Va., March 31, 1975.

REFERENCES

1. Crews, John H., Jr.: An Elastoplastic Analysis of a Uniaxially Loaded Sheet With an Interference-Fit Bolt. NASA TN D-7748, 1974.

2. Isakson, G.; Armen, H., Jr.; and Pifko, A.: Discrete-Element Methods for the Plastic Analysis of Structures. NASA CR-803, 1967.

3. Armen, H., Jr.; Pifko, A.; and Levine, H. S.: Finite Element Analysis of Structures in the Plastic Range. NASA CR-1649, 1971.

4. Ramberg, Walter; and Osgood, William R.: Description of Stress-Strain Curves by Three Parameters. NACA TN 902, 1943.

5. Crews, John H., Jr.: An Elastic Analysis of Stresses in a Uniaxially Loaded Sheet Containing an Interference-Fit Bolt. NASA TN D-6955, 1972.

6. Howland, R. C. J.: On the Stresses in the Neighbourhood of a Circular Hole in a Strip Under Tension. Phil. Trans. Roy. Soc. (London), ser. A, vol. 229, no. 671, Jan. 6, 1930, pp. 49-86.

7. Bowden, F. P.; and Tabor, D.: The Friction and Lubrication of Solids. Part II. Clarendon Press (Oxford), 1964.

8. Stulen, F. B.; and Cummings, H. N.: A Failure Criterion for Multi-Axial Fatigue Stresses. American Soc. Testing Mater. Proc., vol. 54, 1954, pp. 822-835.

9. Findley, William N.: Experiments in Fatigue Under Ranges of Stress in Torsion and Axial Load From Tension to Extreme Compression. American Soc. Testing Mater. Proc., vol. 54, 1954, pp. 836-852.

10. Little, R. E.: Fatigue Stresses From Complex Loadings. Mach. Des., vol. 38, Jan. 6, 1966, pp. 145-149.

11. Smith, Clarence R.: Interference Fasteners for Fatigue-Life Improvement. Exp. Mech., vol. 5, no. 8, Aug. 1965, pp. 19A-23A.

12. Mead, Daniel R.: Taper-Lok Reference Manual. Second ed., Briles Manufacturing, c.1967.

TABLE 1.- TEST RESULTS FOR A RANGE OF INTERFERENCE

LEVELS WITH $S_{max} = 275$ MPa, $R = 0.05$

Interference level, I, mm	Fatigue life, N, cycles	[a]Crack-initiation site, deg	[a]Location of fretting mark, deg	Median fatigue life, cycles
0	21 090	15	(b)	41 455
	24 830	13	(b)	
	58 080	2	10	
	117 180	0	(b)	
0.025	111 520	50	46	156 900
	120 840	44	47	
	192 960	46	50	
	273 350	57	52	
0.05	303 680	32	50	532 610
	509 210	43	63	
	556 010	29	61	
	1 819 200	56	60	
0.10	619 950	39	No fretting	1 666 745
	1 452 610	36		
	1 880 880	46		
	5 831 390	25		
0.15	635 660	30	No fretting	3 329 355
	2 916 860	32		
	3 741 850	27		
	>12 973 170	---		
0.20	705 480	27	No fretting	1 612 130
	760 710	29		
	2 463 550	31		
	5 703 230	[c]11		
0.25	761 060	29	No fretting	5 447 780
	5 004 480	40		
	5 891 080	34		
	6 354 690	[c]1		
0.30	546 260	24	No fretting	2 669 190
	598 270	27		
	4 740 110	[c]3		
	5 792 900	[c]1		

[a]Angle measured to transverse center line through bolt hole.

[b]Center of fretting mark could not be measured — mark was broad and poorly defined.

[c]Crack initiated on outer edge of specimen.

TABLE 2.- TEST RESULTS FOR I = 0.05 AND 0.10 mm, R = 0.05

Interference level, I, mm	Maximum stress, S_{max}, MPa	Fatigue life, N, cycles	[a]Crack-initiation site, deg	[a]Location of fretting mark, deg	Median fatigue life, cycles
0.05	500	10 620	23	33	11 325
		12 030	8	38	
0.05	450	18 960	7	34	22 235
		25 510	30	32	
0.05	400	35 370	0	44	51 330
		67 290	45	52	
0.05	350	56 150	0	48	102 590
		102 590	29	51	
		265 680	39	50	
0.05	275	303 680	32	50	532 610
		509 210	43	63	
		556 010	29	61	
		1 819 200	56	60	
0.05	250	1 127 210	30	56	9 142 505
		7 951 400	38	63	
		>10 333 610	---	---	
		>10 339 520	---	---	
0.10	500	15 440	31	54	15 460
		15 460	32	50	
		33 870	16	49	
0.10	450	17 410	1	52	42 260
		42 260	3	55	
		60 160	13	56	
0.10	350	194 390	23	66	296 240
		296 240	21	68	
		311 950	32	62	
0.10	275	619 950	39	No fretting	1 666 745
		1 452 610	36		
		1 880 880	46		
		5 831 390	25		
0.10	250	1 016 340	33	No fretting	3 938 925
		1 052 840	25		
		6 825 010	26		
		>10 331 740	---	---------	

[a]Angle measured to transverse center line through bolt hole.

TABLE 3.- FATIGUE RESULTS FOR UNNOTCHED
7075-T6 SPECIMENS, R = 0.05

Maximum stress, S_{max}, MPa	Fatigue life, cycles	Median fatigue life, cycles
517	15 350 17 390 18 990	17 390
483	13 370 18 870 19 300 23 170	19 085
414	21 830 22 520 30 710 37 980	26 615
379	27 360 36 190 43 070 47 130	39 630
345	68 800 216 880 595 500	216 880
310	339 500 3 395 100 3 500 830	3 395 100
296	2 575 620 4 140 150 7 495 000	4 140 150
275	8 530 170 >10 052 200 >10 082 370	>10 052 200

14

TABLE 4.- FATIGUE-TEST RESULTS FOR 7075-T6 SHEET

SPECIMENS WITH OPEN HOLES,   R = 0.05

Maximum stress, S_{max}, MPa	Fatigue life, cycles	Median fatigue life, cycles
552	650 700	675
483	1 100 1 220	1 160
414	3 040 4 350	3 695
345	5 920 6 020	5 970
275	12 680 13 060 13 100 29 180	13 080
207	36 200 41 620 52 080	41 620
172	228 760 3 657 110 8 434 630	3 657 110
156	1 681 887 8 598 090 >10 085 956 >10 565 690	>9 342 023
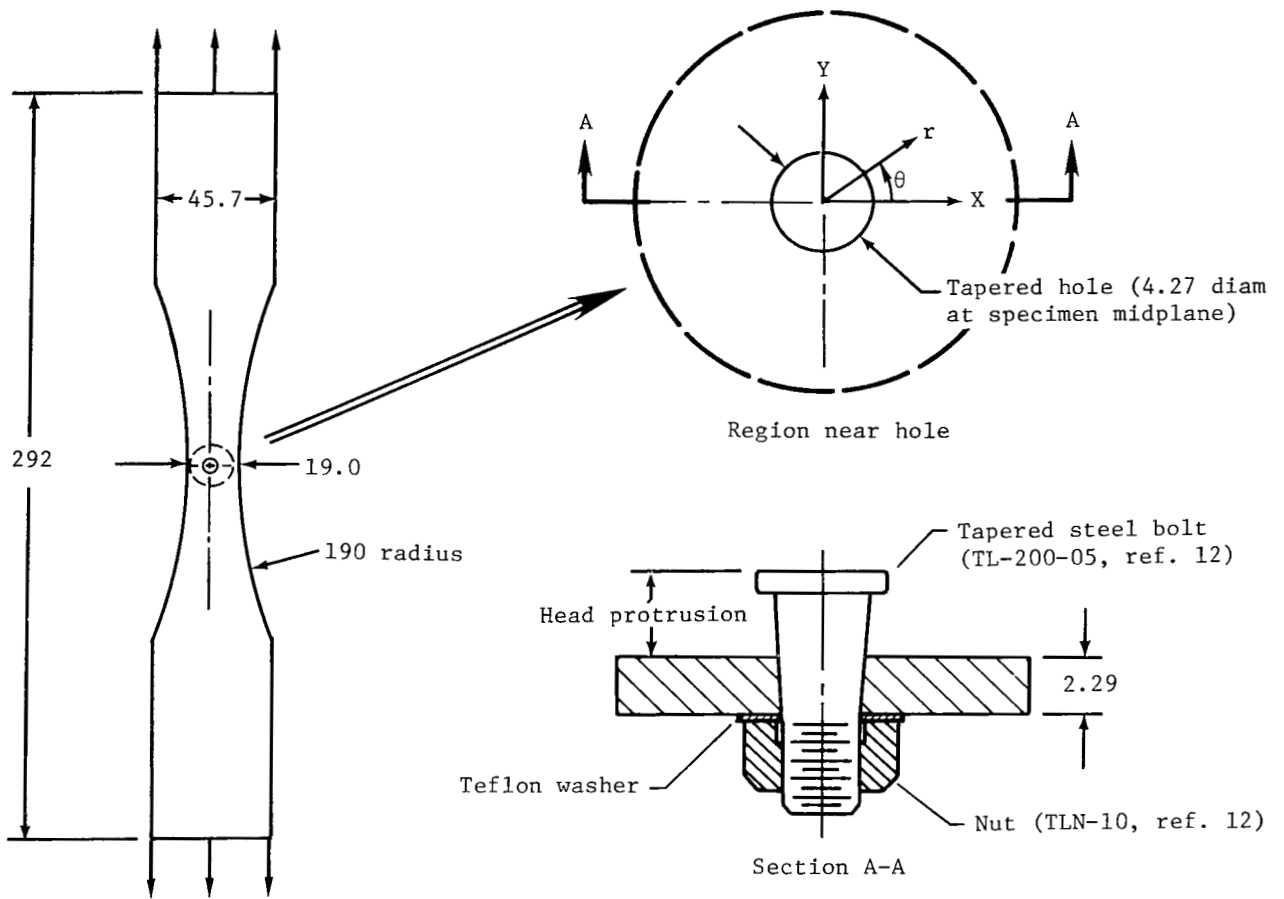
Figure 1.- Fatigue specimen with interference-fit bolt.
Materials: 7075-T6 aluminum-alloy specimen,
steel bolt.   (Dimensions in millimeters.)
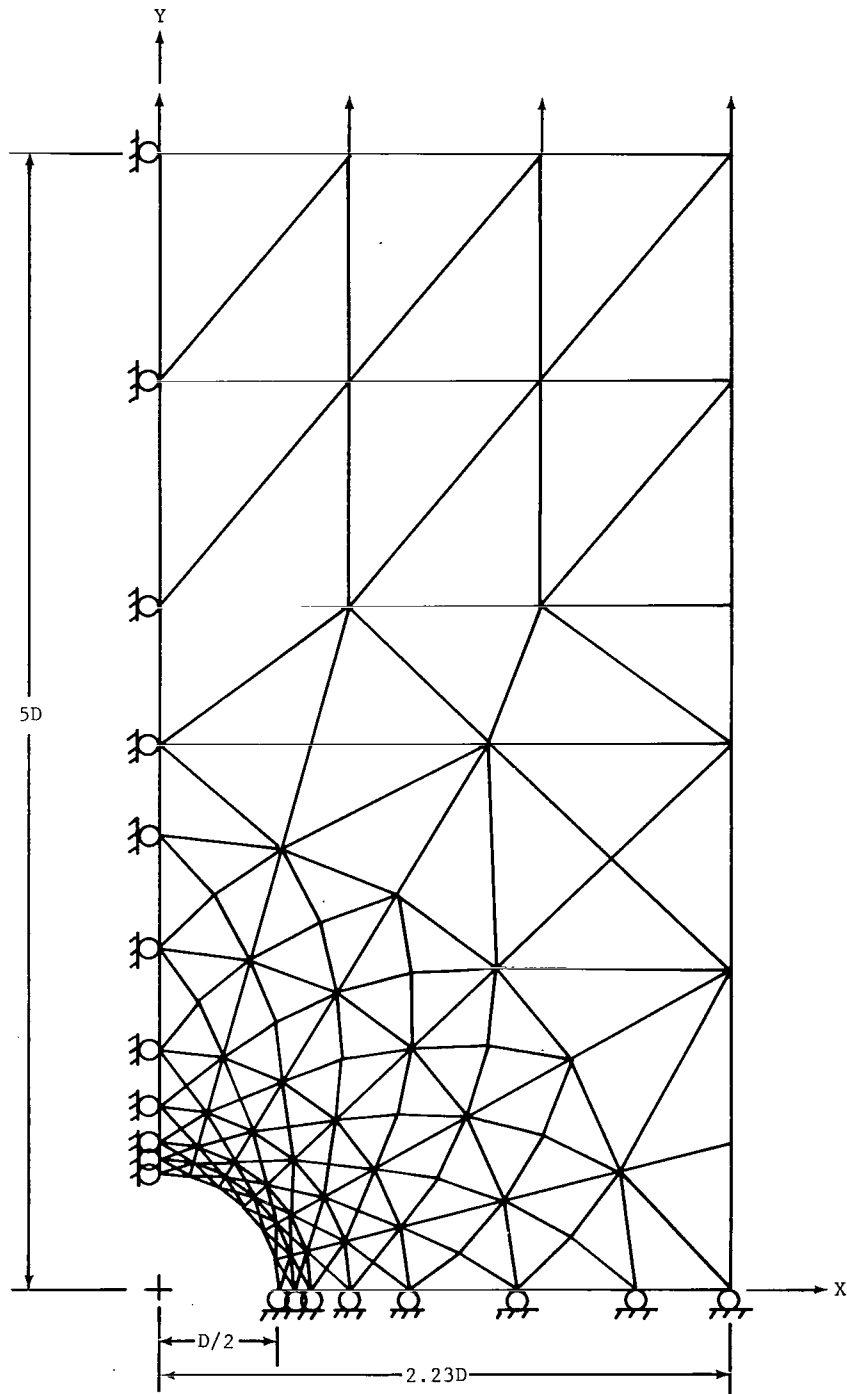
(a) Fatigue specimen.

Figure 2.- Finite-element idealization for one quandrant
of fatigue specimen and bolt.

17
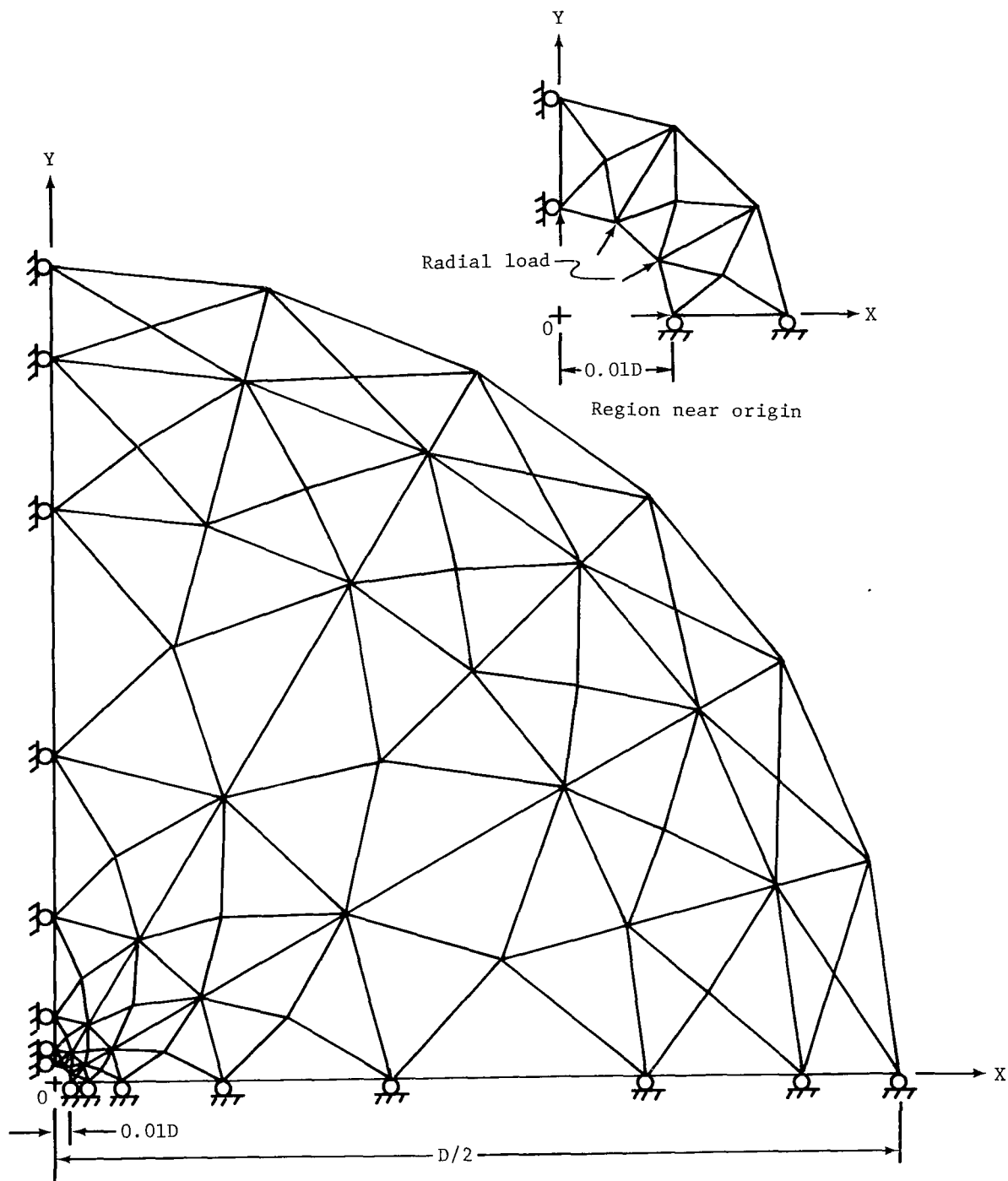
(b) Bolt.

Figure 2.- Concluded.
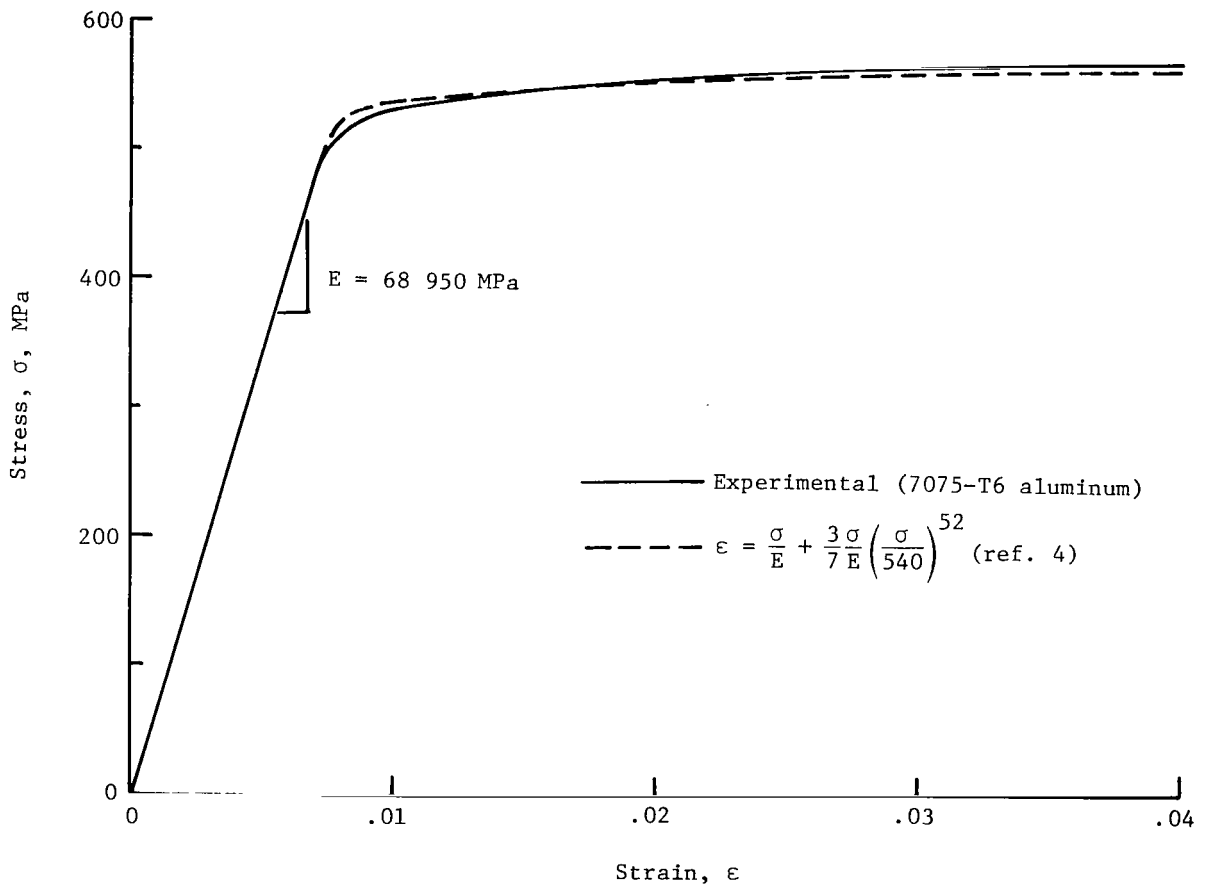
Figure 3.- Stress-strain curves.
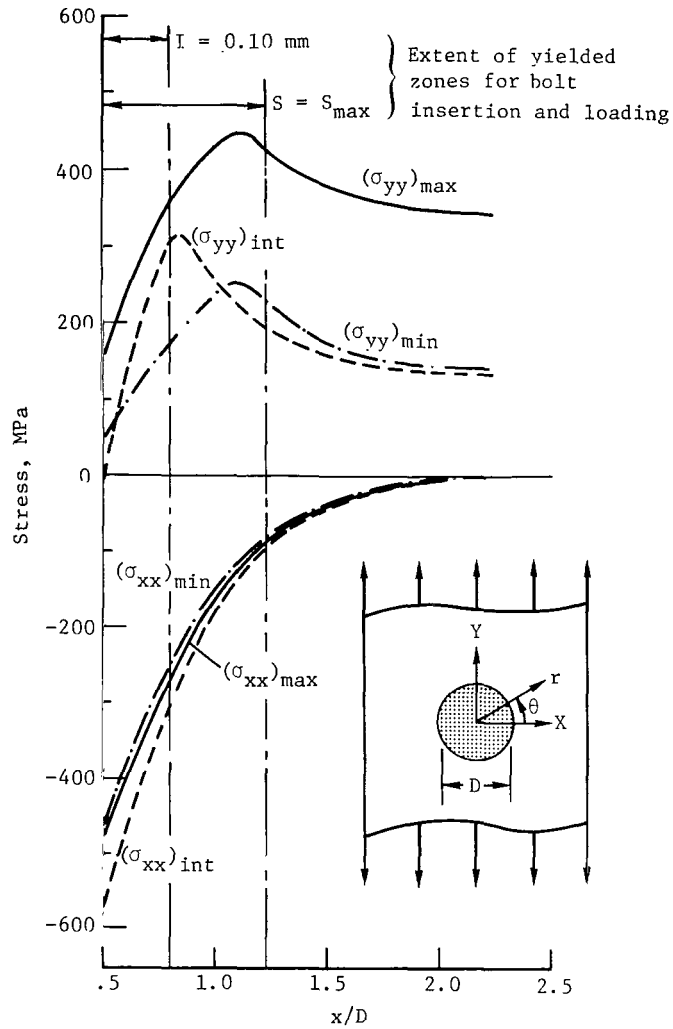
(a) Stress distribution on X-axis.
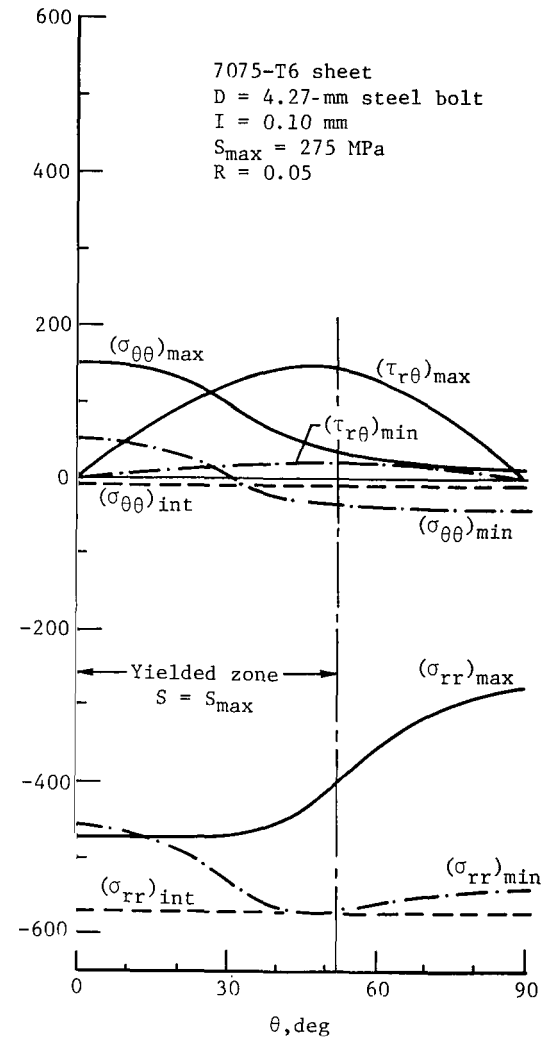
(b) Stress distribution on hole boundary.

Figure 4.- Stress distributions for a specimen with an interference-fit bolt.
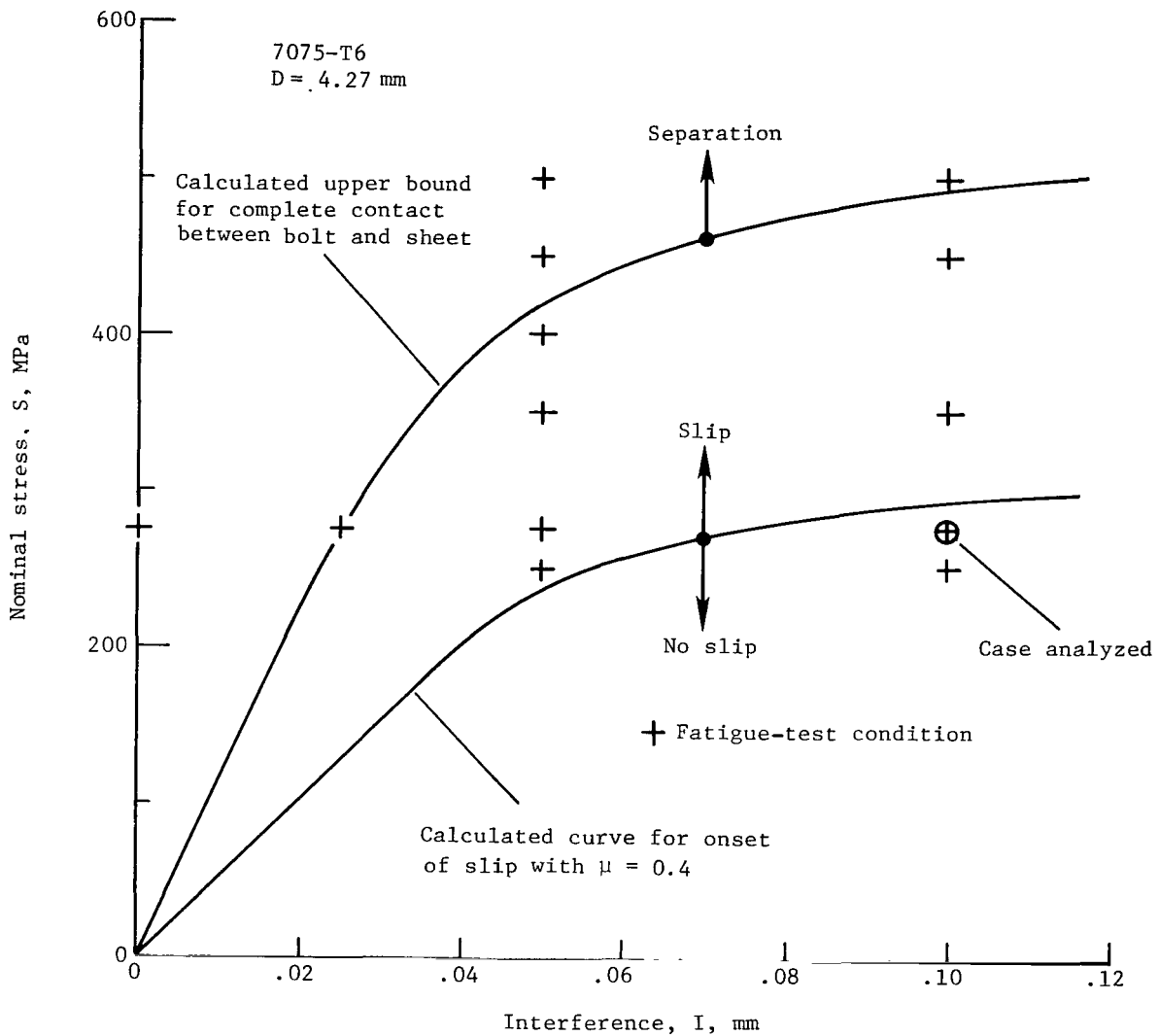
Figure 5.- Comparison of fatigue-test conditions with
calculated slip and separation conditions.
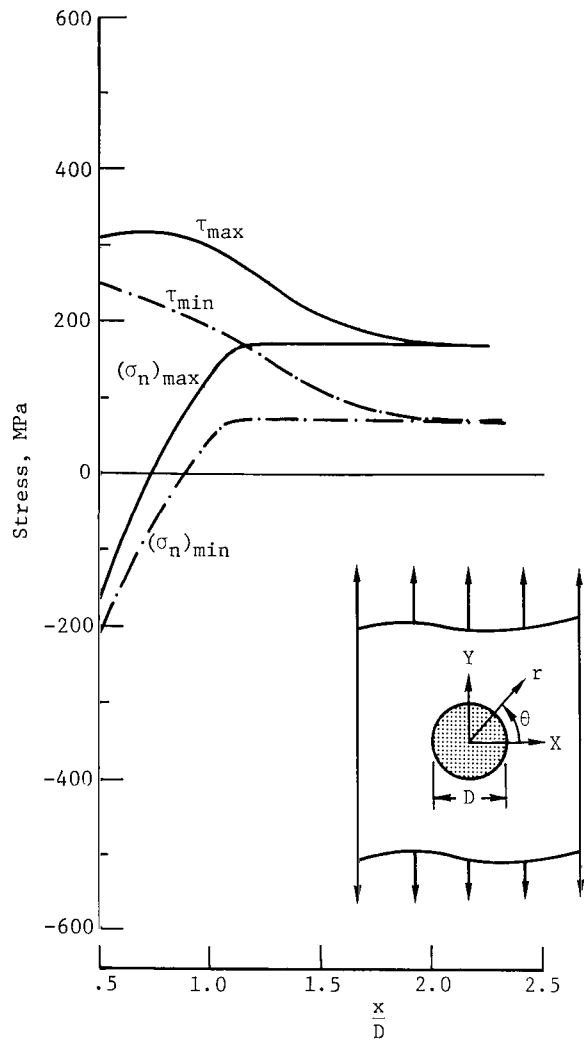
(a) Stress distribution on X-axis.
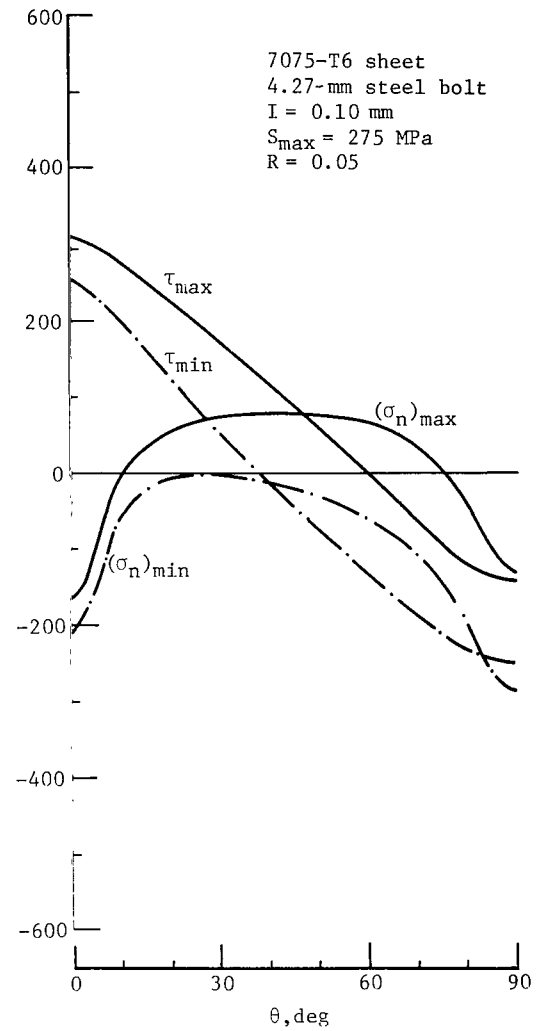
(b) Stress distributions on hole boundary.

Figure 6.- Shear and normal stresses on the planes of maximum alternating shear stress.

100

Alternating shear stress, τ_a, MPa

Y
r
θ
X
D

$N = 10^6$
$N = 10^7$

Constant-life curves
for 7075-T6 sheet, uniaxial
loading, unnotched specimens
(ref. 11)

0.8
0.9
1.0
0.7
0.6

50

$\dfrac{x}{D} \geqslant 1.10$

$\begin{cases} S_{max} = 275 \text{ MPa} \\ I = 0.10 \text{ mm} \\ R = 0.05 \end{cases}$

$\dfrac{x}{D} = 0.5$

0

-200   -100   0   100   200

Maximum normal stress, $(\sigma_n)_{max}$, MPa
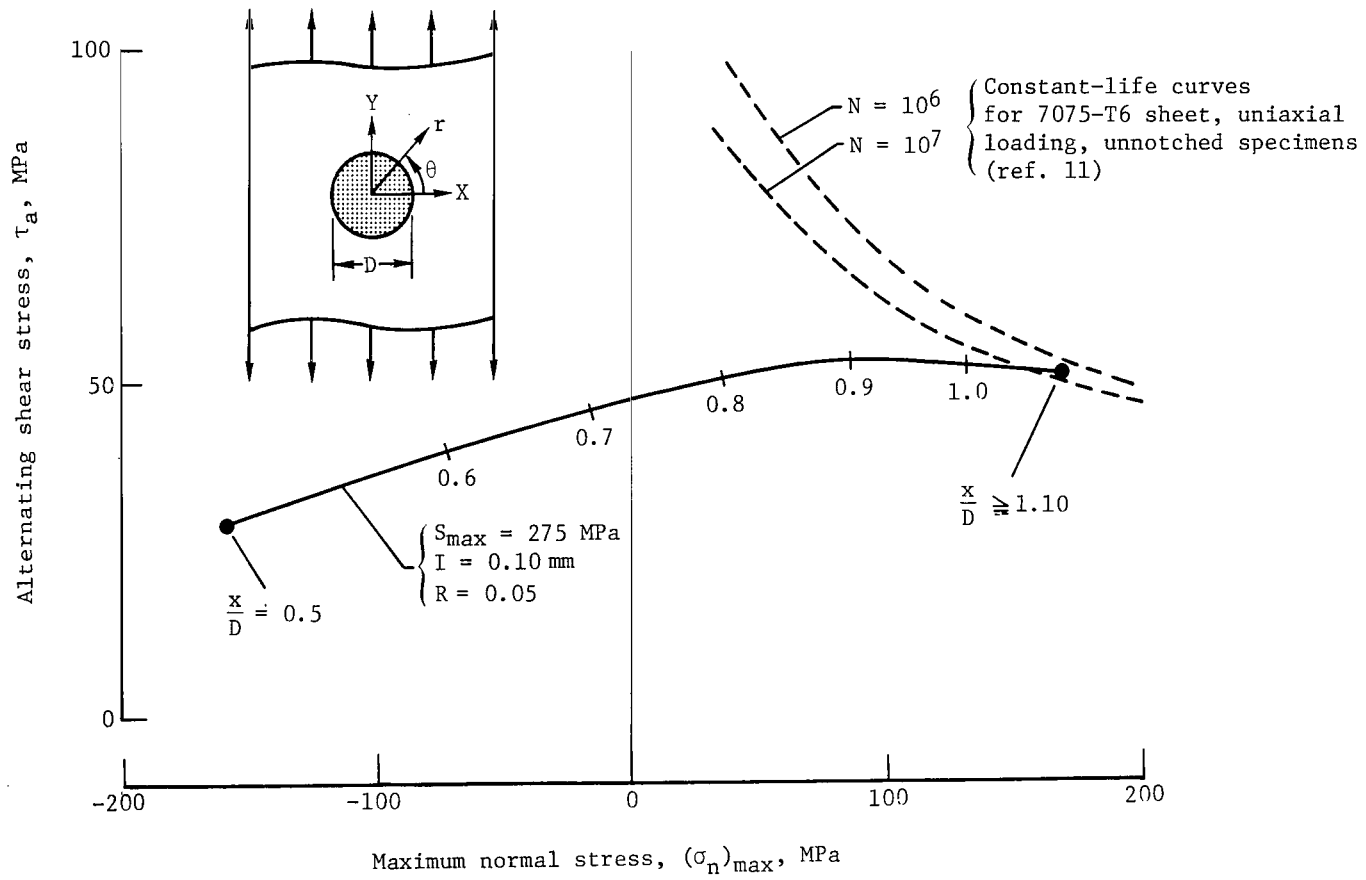
Figure 7.- Comparison of stresses along the X-axis with stresses that cause
fatigue failures in unnotched specimens.
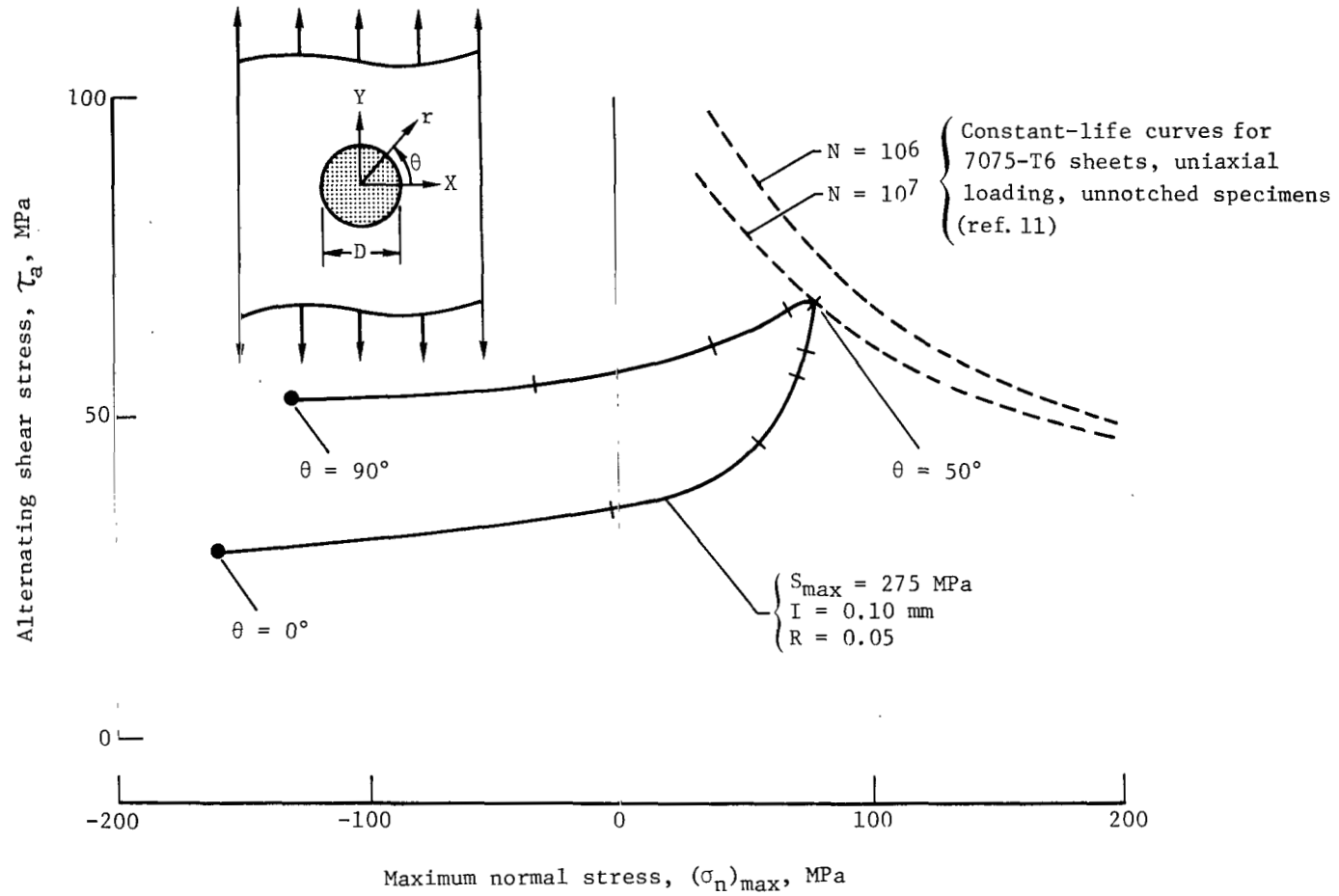
Figure 8.- Comparison of stresses along hole boundary with stresses that cause fatigue failures in unnotched specimens.
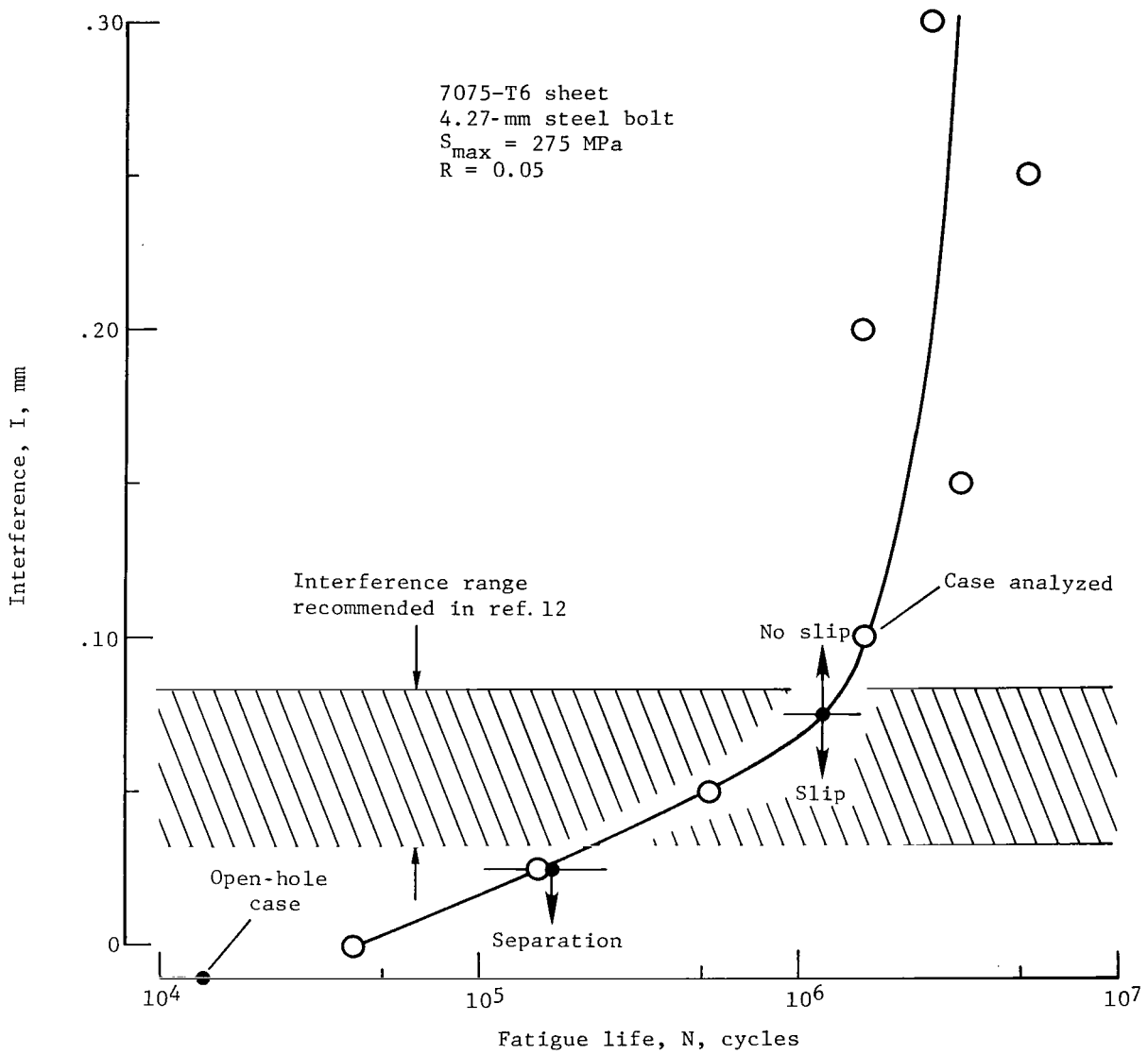
Figure 9.- Influence of interference level on fatigue life.
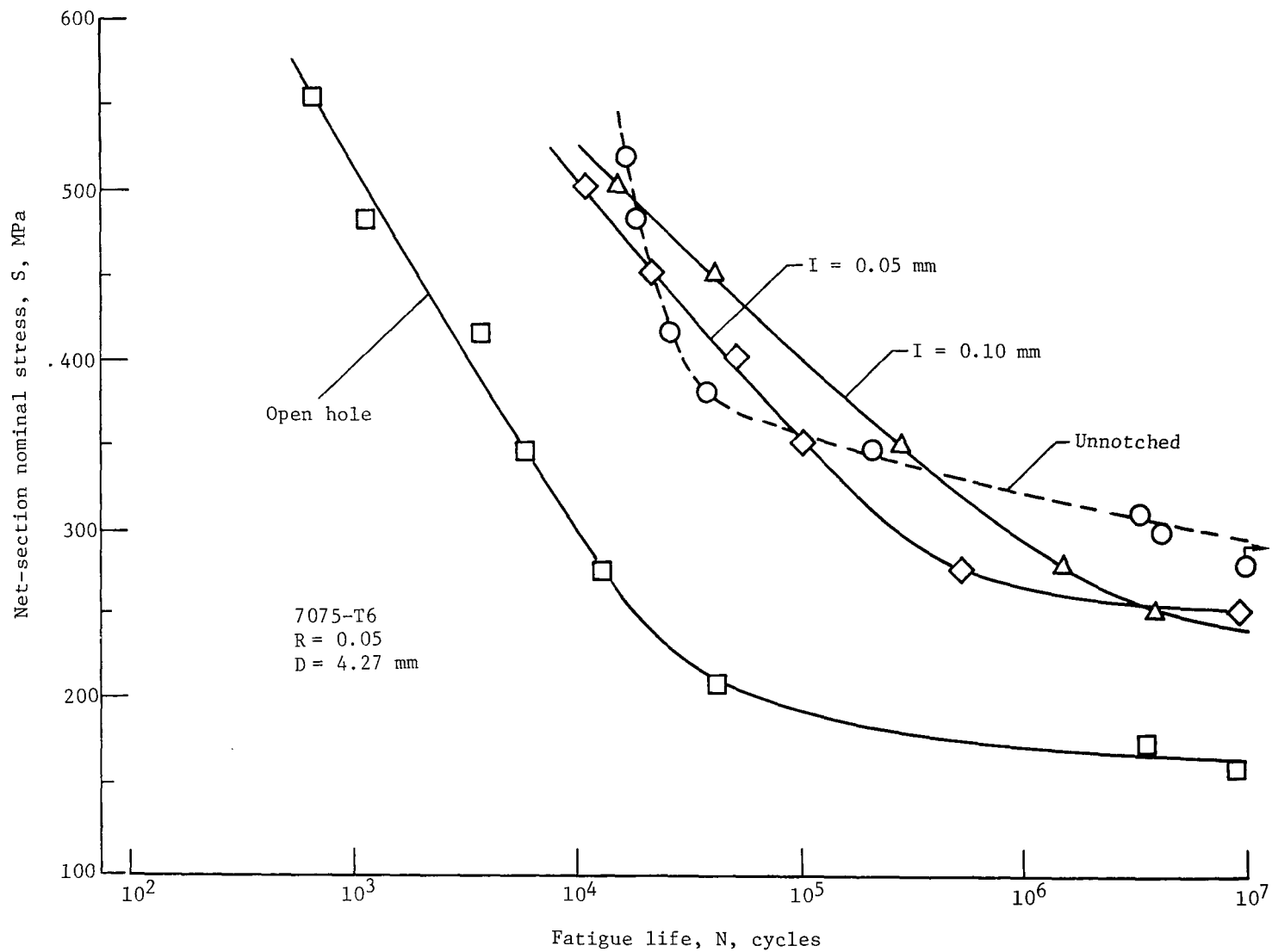
Figure 10.- SN curves based on net-section nominal stress.
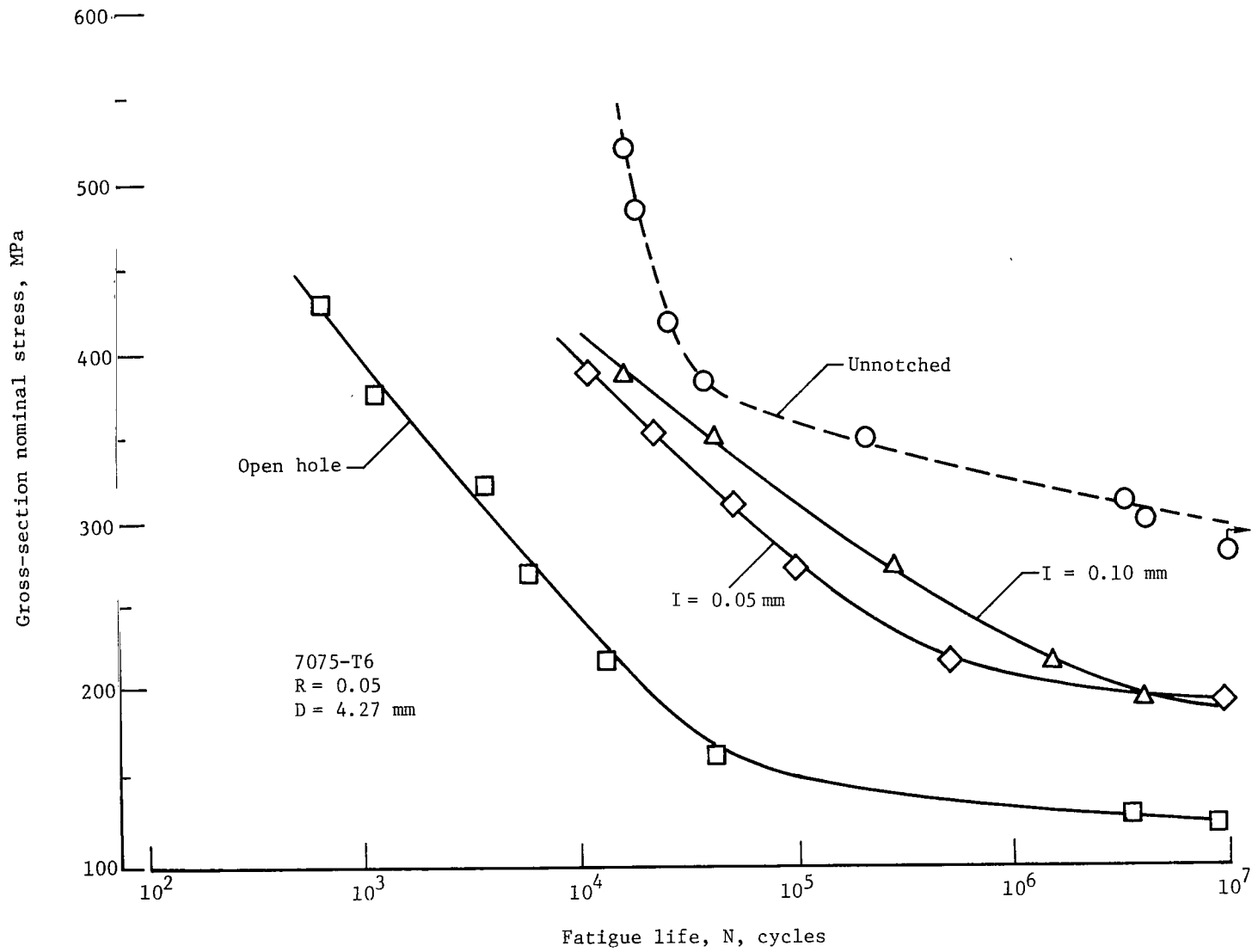
Figure 11.- SN curves based on gross-section nominal stress.
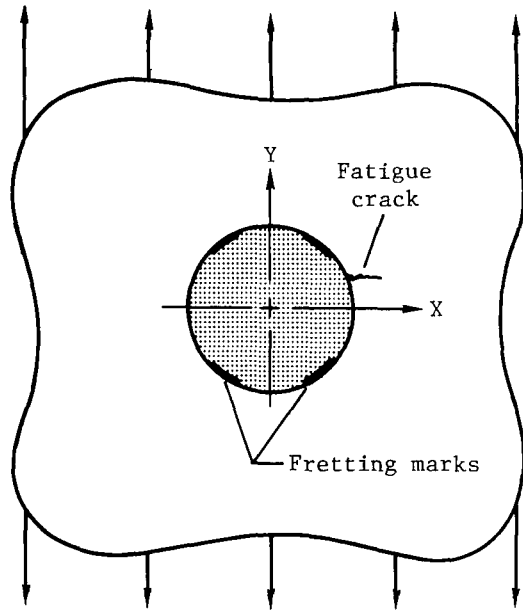
(a) Typical locations for fatigue
cracks and fretting marks.
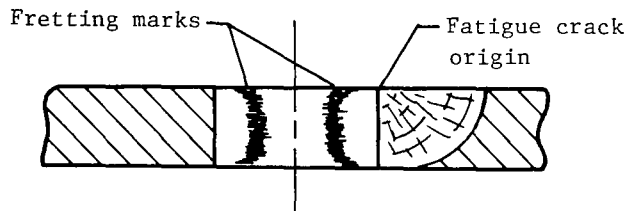
(b) Typical fracture surface.
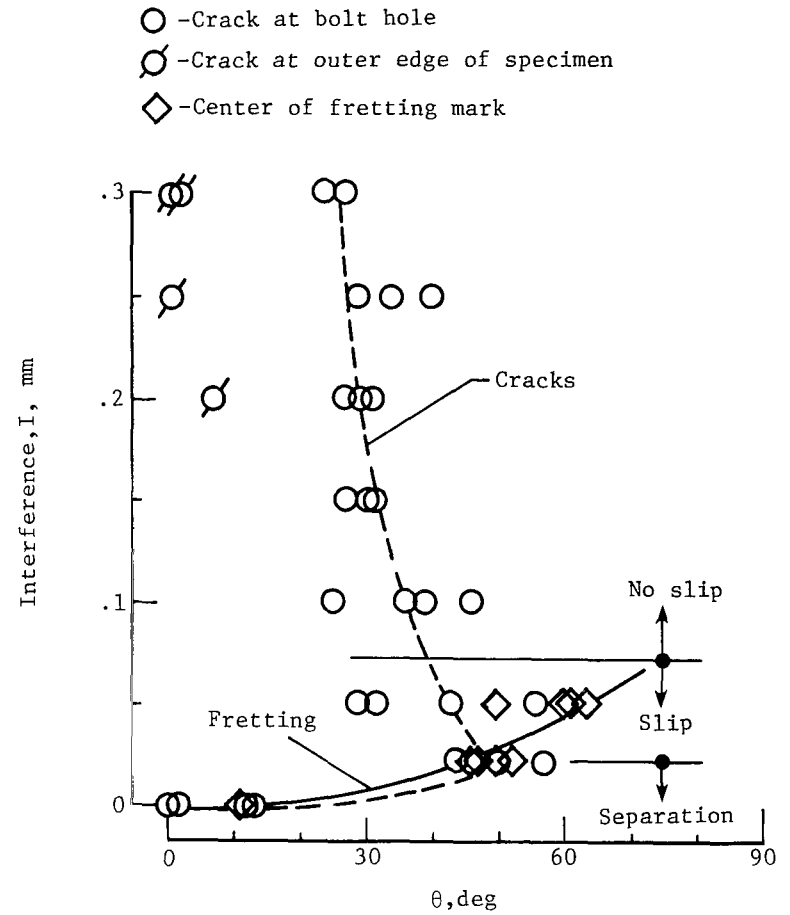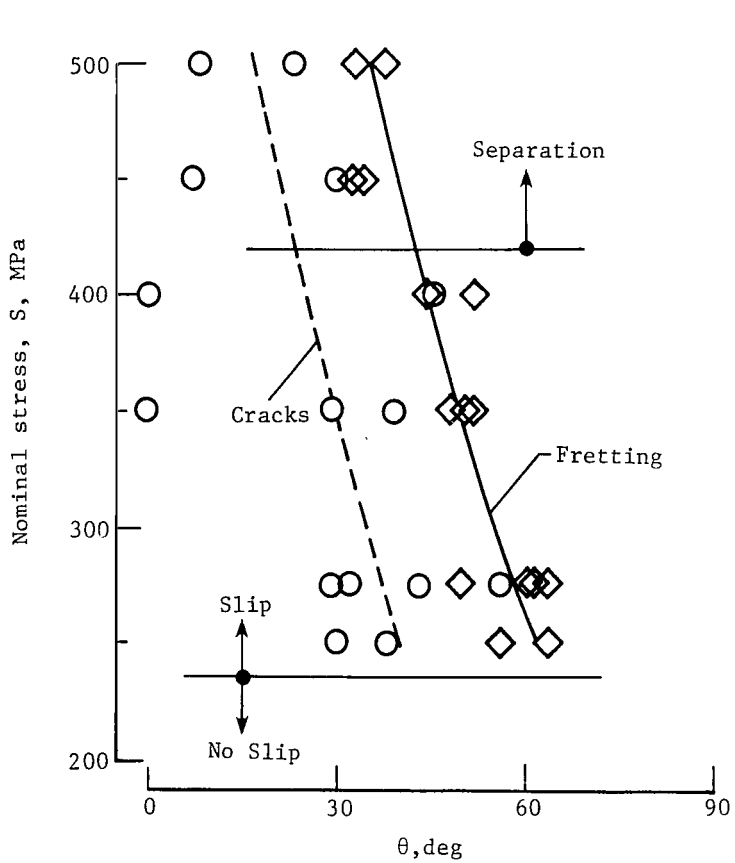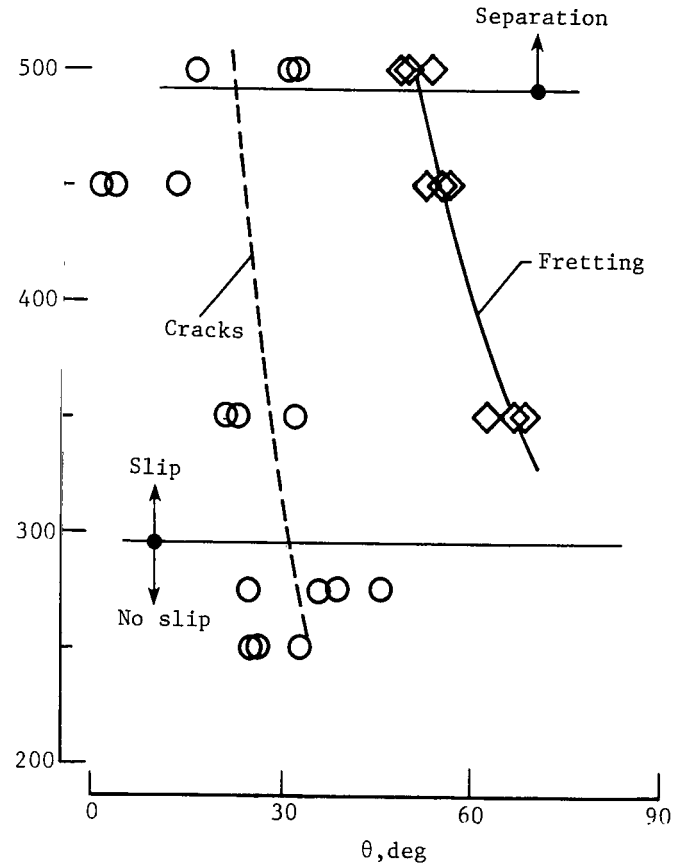
(c) Test results for S_{max} = 275 MPa.

Figure 12.- Locations for fatigue cracks and fretting marks in bolt hole.

(d) Test results for I = 0.05 mm.

(e) Test results for I = 0.10 mm.

Figure 12.- Concluded.

*"The aeronautical and space activities of the United States shall be
conducted so as to contribute . . . to the expansion of human knowl-
edge of phenomena in the atmosphere and space. The Administration
shall provide for the widest practicable and appropriate dissemination
of information concerning its activities and the results thereof."*

—NATIONAL AERONAUTICS AND SPACE ACT OF 1958

NASA SCIENTIFIC AND TECHNICAL PUBLICATIONS

TECHNICAL REPORTS: Scientific and
technical information considered important,
complete, and a lasting contribution to existing
knowledge.

TECHNICAL NOTES: Information less broad
in scope but nevertheless of importance as a
contribution to existing knowledge.

TECHNICAL MEMORANDUMS:
Information receiving limited distribution
because of preliminary data, security classifica-
tion, or other reasons. Also includes conference
proceedings with either limited or unlimited
distribution.

CONTRACTOR REPORTS: Scientific and
technical information generated under a NASA
contract or grant and considered an important
contribution to existing knowledge.

TECHNICAL TRANSLATIONS: Information
published in a foreign language considered
to merit NASA distribution in English.

SPECIAL PUBLICATIONS: Information
derived from or of value to NASA activities.
Publications include final reports of major
projects, monographs, data compilations,
handbooks, sourcebooks, and special
bibliographies.

TECHNOLOGY UTILIZATION
PUBLICATIONS: Information on technology
used by NASA that may be of particular
interest in commercial and other non-aerospace
applications. Publications include Tech Briefs,
Technology Utilization Reports and
Technology Surveys.

Details on the availability of these publications may be obtained from:

SCIENTIFIC AND TECHNICAL INFORMATION OFFICE

NATIONAL AERONAUTICS AND SPACE ADMINISTRATION

Washington, D.C. 20546